# Phonon anomalies in transition-metal nitrides: ZrN

A. N. Christensen
*Department of Inorganic Chemistry, Aarhus University, DK-8000 Aarhus C, Denmark*

O. W. Dietrich
*Department of Physics, Risø National Laboratory, DK-4000 Roskilde, Denmark*

W. Kress
*Max-Planck-Institut für Festkörperforschung, D-7 Stuttgart, Federal Republic of Germany*

W. D. Teuchert
*Department of Physics E21, Technische Universität München, D-8 München 2, Federal Republic of Germany*
(Received 20 November 1978)

The phonon dispersion curves in superconducting ZrN have been measured in the high-symmetry directions $\Delta$, $\Sigma$, and $\Lambda$ by coherent inelastic neutron scattering at room temperature. Anomalies in the dispersion of the acoustic branches have been detected which are similar to those reported already for the superconducting transition-metal carbides and for TiN. The experimental results are well reproduced by a double-shell model which has also been used to calculate the phonon density of states. The calculated density is in good agreement with the results of time-of-flight measurements and with recent Raman data.

## I. INTRODUCTION

The carbides and nitrides of the groups IV, V, and VI transition metals exhibit a unique combination of covalent properties like high bonding strength and high melting points with metallic properties such as appreciable thermal and electrical conductivity and metallic luster. The compounds are hard and brittle. Some of the transition-metal carbides and nitrides are superconductors with $T_c$ values up to 18 K.[1,2] These fairly high $T_c$ values indicate a strong electron-phonon interaction. It is therefore of great interest to investigate the phonon spectra of these compounds. In recent years lattice dynamics of transition-metal carbides has been intensively studied both experimentally[3–7] and theoretically.[8–19] It has been found that some of the transition-metal carbides which are superconductors show anomalies in the phonon dispersion curves whereas those which are not superconductors do not exhibit these additional structures. Theoretical investigations[14–19] have shown that both the phonon anomalies as well as the high superconducting transition temperatures originate from a resonance-like increase of the dielectric screening. In a recent paper[20] we have shown that TiN exhibits anomalies which are even more pronounced than those for the isoelectronic carbide NbC. The present paper extends our investigation of transition-metal nitrides to ZrN.

## II. EXPERIMENTAL

A single crystal of ZrN was prepared by a zone annealing technique.[21] A zirconium rod of nominal 99.99% purity was zone annealed in a nitrogen atmosphere of nominal 99.99% purity under a pressure of 2 MPa at a temperature of approximately 2800 °C. The composition of the crystal was determined gravimetrically by ignition of ZrN in air of 1180 °C to $ZrO_2$. The composition of the single crystal used in the neutron scattering experiments was $ZrN_{0.93}$. The lattice constant of the specimen was determined from a Guinier powder pattern using Cu $K\alpha_1$ radiation to be $a = 4.574(1)$ Å. The density was measured by the method of Archimedes and was $\delta_m = 7.327$ g cm$^{-3}$. The sample used in the inelastic coherent neutron scattering experiments was cylindrical in shape with diameter 11 mm and length 32 mm.

The phonon dispersion curves were measured in the high-symmetry directions $\Delta$, $\Sigma$, and $\Lambda$. All measurements were performed at room temperature in a scattering plane perpendicular to the $[\bar{1}10]$ axis. The acoustic branches of the phonon dispersion curves were measured on a triple axis spectrometer at the DR3 reactor at Risø National Laboratory. A combination of different measuring techniques such as variable incoming neutron energy and fixed outgoing energy, or fixed incoming neutron energy and variable outgoing energy (monochromator and analyzer

 

scans) was used. The optic branches were measured on the triple-axis spectrometer IN1 situated at the hot source of the high-flux reactor of the Institut Laue-Langevin. The scans were performed at constant incident neutron energy and mainly at constant wave-vector transfer $Q$. Due to the high incoherent background from the sample and the IN1 hot-source spectrum spurious scattering processes were observed up to high orders. Care was taken to avoid superpositions of the desired phonon peak with any spurious scattering events by frequent changes of the incident energy. Comparison scans were performed at nearby wave vectors $Q$ where no coherent processes could contribute in order to assess the background scattering originating from the density of states via incoherent scattering. In addition, constant energy-transfer scans were used where the dispersion curves are steep enough to give well defined peaks. In this case the incoherent scattering is merely a smoothly varying background with the coherent one-phonon peak standing out clearly on top of it. The results of the measurements are shown in Fig. 1. At the bottom of the figure is shown a mapping of the measured relative intensities of the acoustic phonons measured in odd and even zones.

## III. MODEL CALCULATIONS

The measured data have been analyzed in terms of a double-shell model[10] which had already been used to reproduce the measured data of the transition-metal carbides and those of TiN. In the model, force constants to first $A_{12}$, $B_{12}$ and second $A_{11}, B_{11}, A_{22}, B_{22}$ nearest neighbors (1 labels the nitrogen ions, 2 labels the metal ions) are taken into account. These forces are assumed to act only via the shells. The shells are coupled to their own cores by the force constants $K_1$ and $K_2$ and carry the charges $Y_1$ and $Y_2$. The ionic charges are $Z_1$ and $Z_2$. This leads in the adiabatic approximation to the well-known equation of motion of the shell model

$$\underline{m}\,\omega^2\underline{U} = [\underline{R} + \underline{ZCZ} - (\underline{R} + \underline{ZCY}) \times (\underline{K} + \underline{R} + \underline{YCY})^{-1}(\underline{R} + \underline{YCZ})]\underline{U}\ , \qquad (1)$$

where $\underline{m}$, $\underline{Z}$, $\underline{Y}$, and $\underline{K}$ are diagonal matrices of the masses, the ionic charges, and the core-shell force constants, respectively. The screening due to the conduction electrons has to be taken into account by adding the term $\underline{D}^{sc}\underline{u}$ to the right-hand side of Eq.(1).

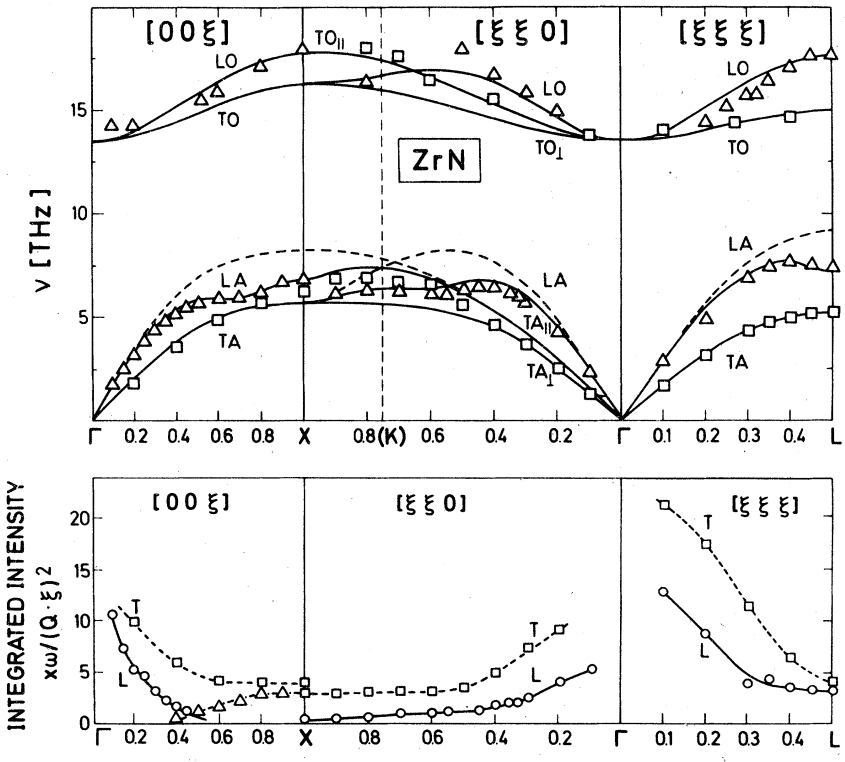


FIG. 1. Acoustic and optic phonons of $ZrN_{0.93}$. Squares and triangles represent the experimental data for transverse and longitudinal phonons, respectively. The solid and dashed lines are the results of calculations using a double-shell model and a simple-shell model, respectively. At the bottom is shown a mapping of the measured relative intensities of the acoustic phonons measured in odd and even zones.

$\underline{D}^{sc}$ is given by

$$D^{sc}_{\alpha\alpha'}(q,KK') = 4\pi Z_S^K Z_S^{K'} \frac{q_\alpha q_\beta}{q^2}\left(\frac{1}{\epsilon(q)} - 1\right), \quad (2)$$

where $\epsilon(q)$ is the dielectric function which is calculated in the Thomas-Fermi approximation, and $Z_S^K$ are the screening charges.

The coupling of the conduction electrons in the metal sublattice is described by force constants $A_{22}^{(1)}, B_{22}^{(1)}, C_{22}^{(1)}$ to first and $A_{22}^{(2)}, B_{22}^{(2)}$ to second nearest neighbors in the metal sublattice. These forces are assumed to act through an outer shell of the metal ions which is coupled by the force constant $K'$ to the inner shell of the metal ions. This additional electronic degree of freedom is taken into account by replacing the short-range matrix $\underline{R}$ in Eq. (1) by the renormalized matrix

$$\tilde{\underline{R}} = \underline{R} + \underline{K}'(\underline{K}' + \underline{R}')^{-1}\underline{R}',$$

where $\underline{R}'$ is the short-range matrix for the additional coupling in the metal sublattice and $K'$ is the diagonal matrix of the coupling between inner and outer shells. It is obvious that the renormalization leads to a sharp resonance-like softening when $\underline{K}'$ and $\underline{R}'$ have different signs and the denominator $\underline{K}' + \underline{R}'$ becomes small. The sharpness of the resonance depends on $K'$ whereas its position in $q$ space depends on the ratio of first- and second-nearest-neighbor forces in the metal sublattice. If only second-neighbor interactions are assumed the softening in the $\Delta$ direction will occur at $0.5(1,0,0)$. If in addition nearest neighbors are mixed in, it will be shifted towards the zone boundary where it will occur when nearest-neighbor forces are much stronger than second-nearest-neighbor forces.

The parameters of the model have been determined by a least-squares fit to the measured data and are compared in Table I with the parameters obtained for TiN.

## IV. RESULTS AND DISCUSSION

In Fig. 1 the measured data are compared to the results of model calculations. Squares and triangles represent the experimental data for transverse and longitudinal phonons, respectively. The solid and dashed lines are the results of calculations using a double-shell model and a simple-shell model, respectively. The experimental data are well reproduced by the calculations using a double shell model. The difference between the full curves and the dashed curves exhibits clearly the softening of the longitudinal branches which has also been found in the superconducting carbides.[3–6] Compared to TiN,[20] the anomalies in ZrN are less pronounced, i.e., the softening is weaker and extends over a larger region in $q$ space. This has to be attributed to the difference in stoichiometry of the two samples ($ZrN_{0.93}$ compared to $TiN_{0.98}$). It is well known that the superconducting properties depend strongly on the number of valence electrons per elementary cell. Transition metal compounds with eight valence electrons (VE) per elementary cell are not superconducting whereas those with nine and ten VE are superconducting and show anomalies in the dispersion curves. This behavior does not depend on whether the change in VE per elementary cell is due to changes in the metal component, the nonmetal component or the stoichiometry. The transition temperature is a monotonous function of the stoichiometry and therefore of the number of VE. This can be understood in a rigid-band model which has been proved to be a reasonable first approximation for the electronic structure by various band-structure calculations.[22–24] In

TABLE I. Double-shell model parameters of ZrN and TiN. Force constants are given in units of $e^2/2r_0^3$, screening vectors are given in units of $\pi/r_0$. The subscripts 1 and 2 refer to the nonmetal and metal sublattice, respectively. The superscripts $n$ refer to the $n$th-order neighbors in the fcc metal sublattice.

| | $A_{12}$ | $B_{12}$ | $A_{22}$ | $B_{22}$ | $A_{11}$ | $B_{11}$ | $Z_1$ | $K_2$ |
|---|---|---|---|---|---|---|---|---|
| ZrN | 15.51 | 1.12 | 10.68 | −2.71 | 2.29 | 0.57 | −0.62 | 300.00 |
| TiN | 18.53 | 1.92 | 11.65 | −3.18 | ··· | ··· | −0.70 | 41.60 |
| | $A_{22}^{(1)}$ | $B_{22}^{(1)}$ | $C_{22}^{(1)}$ | $A_{22}^{(2)}$ | $B_{22}^{(2)}$ | $K'$ | $k_F$ | $k_S$ |
| ZrN | −1.108 | 0.140 | −0.097 | −0.696 | 0.4509 | 5.0 | 0.3 | 0.3 |
| TiN | −0.399 | −0.094 | −0.043 | −0.411 | 0.0213 | 1.9 | 0.5 | 0.5 |

$Y_1 = Y_2 = 0$ $\quad K_1 = \infty$

this picture the Fermi energy lies in a minimum of the electronic density of states for compounds with eight VE and is shifted into a region with increasing density of $d$ states when the number of VE is increased. In a microscopic picture this leads to a strong $p$-$d$ coupling which results in a resonance-like behavior of the dielectric function for certain $q$ vectors.[18,19] It should be mentioned that in contrast to the carbides and to TiN, the TA branch in the $\Sigma$ direction shows no anomaly. From the slopes of the acoustic branches the elastic constants have been determined to be

$$c_{11} = 4.54\ 10^{12}\text{dyn/cm}^2 ,$$

$$c_{12} = 1.21\ 10^{12}\text{dyn/cm}^2 ,$$

and

$$c_{44} = 1.24\ 10^{12}\text{dyn/cm}^2 .$$

Optic and acoustic branches are separated by an energy gap. Because of the screening due to conduction electrons the LO and TO modes are degenerate at the $\Gamma$ point, whereas the splitting of LO and TO modes at the $L$ point is due to the long-range Coulomb interaction which is not completely screened at larger $q$ vectors.

In Table I the parameters of the model for ZrN and TiN are compared. The short-range force constants for both compounds are very similar. The main difference is that for ZrN second-nearest-neighbor interactions in the nitrogen sublattice had to be added. They are, however, small compared to the second-nearest-neighbor forces in the metal sublattice. It should be mentioned that in both compounds the polarizability of the nitrogen ions can be neglected and that in ZrN the polarizability of the Zr ions is much weaker ($K_2$ larger) than the polarizability of the Ti ions in TiN. The less pronounced anomalies lead to a bigger $K'$ value. It is the $K'$ value which essentially describes the localization of the anomalies in $q$ space. The smaller the $K'$ value is the more localized are the anomalies. The coupling constants $A_{22}^{l}/K'$ and $B_{22}^{l}/K'$ describe essentially the magnitude of the softening. In ZrN these quantities are generally smaller than in TiN thus reflecting the weaker softening in ZrN.

In Fig. 2 the calculated one-phonon density of states of the acoustic branches (histogram) is compared with the results from time-of-flight measurements (dotted line) by Gompf[25] on $ZrN_{0.87}$. The overall shape of both spectra is in good agreement. Small differences in the intensity ratios may be due to the fact that the measured density has to be converted into the true phonon density of states by frequency dependent corrections and that the stoichiometry of the samples used in the time-of-flight measurements and the samples used in the present triple-axis experiment was quite different.

In Fig. 3 the calculated density for both the acoustic and the optic branches is compared with the Raman spectrum measured by Spengler and Kaiser[26] on $ZrN_{0.95}$. Again we find good agreement in the acous-

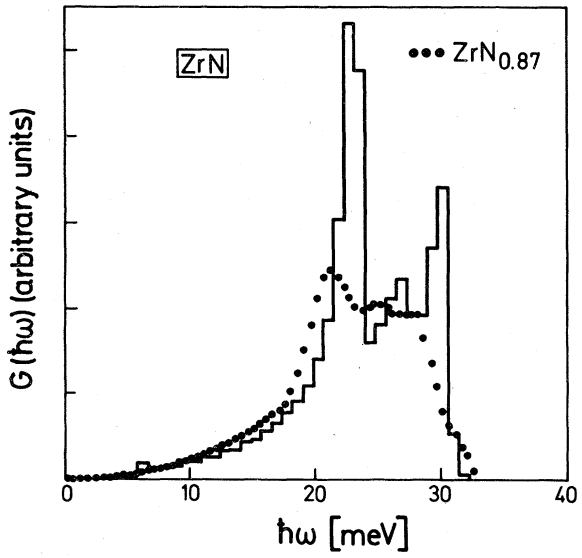


FIG. 2. Histogram of the calculated one-phonon density of states of the acoustic phonons of $ZrN_{0.93}$ compared with the results from time-of-flight measurements on $ZrN_{0.87}$ (Gompf, Ref. 25).

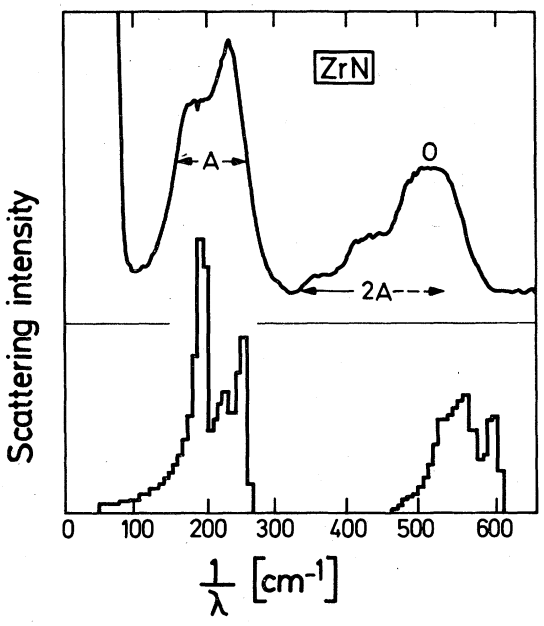


FIG. 3. Histograms of the calculated density of the acoustic and optic phonons of $ZrN_{0.93}$ compared with the Raman spectrum measured on $ZrN_{0.95}$ (Spengler and Kaiser, Ref. 26).

tic part of the spectrum. The calculated density of the optic branches seems to be shifted slightly to higher frequencies compared to the second peak in the experiment. However, there are strong two-phonon contributions of the acoustic branches superposed with the density of the optic branches in this peak. It can be easily imaginated that the subtraction of the two-phonon contribution indicated by the arrow labeled 2A will lead to the calculated density.

## V. CONCLUSIONS

It has been shown that ZrN exhibits similar phonon dispersion curves as the isoelectronic carbides. This is in accordance with the rigid-band picture. Compared to TiN the anomalies are less pronounced which is very likely to be related to the poorer stoichiometry of the ZrN sample. The experimental results are well reproduced within the framework of a double-shell model which has already been used to describe the lattice vibrations in other transition-metal compounds.[10,12,20] The calculated one-phonon density is in good agreement with the results of time-of-flight measurements[25] and with recent Raman measurements.[26]

## ACKNOWLEDGMENTS

We are grateful to Dr. J. Copley for his assistance during the measurements of the optic branches and thank the Institut Laue-Langevin for its hospitality We are grateful to Dr. Gompf for providing us with the density-of-states data prior to publication. One of us (W.K.) acknowledges Professor H. Bilz for valuable discussions. The Danish Natural Science Research Council is acknowledged for financial support to one of us (A.N.C.).

[1]L. E. Toth, *Transition Metal Carbides and Nitrides* (Academic, New York, 1971).
[2]B. W. Roberts, J. Phys. Chem. Ref. Data 5, 581 (1976).
[3]H. G. Smith and W. Gläser, Phys. Rev. Lett. 25, 1611 (1970).
[4]H. G. Smith, in *Superconductivity in d- and f-Band Metals,* edited by D. H. Douglass (AIP, New York, 1972), p. 321.
[5]H. G. Smith and W. Gläser, in *Phonons,* edited by M. A. Nusimovici (Flammarion, Paris, 1972), p. 145.
[6]H. G. Smith, Phys. Rev. Lett. 29, 353 (1972).
[7]F. Gompf, L. Pintschovius, W. Reichardt, and B. Scheerer, in *Proceedings of the Conference on Neutron Scattering,* edited by R. M. Moon (NTIS, Springfield, Virginia, 1976), p. 129.
[8]W. Weber, H. Bilz, and U. Schröder, Phys. Rev. Lett. 28, 600 (1972).
[9]M. Mostoller, Phys. Rev. B 5, 1260 (1972).
[10]W. Weber, Phys. Rev. B 8, 5082 (1973).
[11]W. Weber, Phys. Rev. B 8, 5093 (1973).
[12]J. L. Feldmann, Phys. Rev. B 12, 813 (1975).
[13]M. P. Verma and B. R. K. Gupta, Phys. Rev. B 12, 1314 (1975).
[14]S. K. Sinha and B. N. Harmon, Phys. Rev. Lett. 35, 1515 (1975).
[15]M. Gupta and A. J. Freeman, Phys. Lett A 57, 291 (1976).
[16]M. Gupta and A. J. Freeman, Phys. Rev. Lett. 37, 364 (1976).
[17]M. Gupta and A. J. Freeman, Phys. Rev. B 14, 5205 (1976).
[18]W. Hanke, J. Hafner, and H. Bilz, Phys. Rev. Lett. 37, 1560 (1976).
[19]J. Hafner, W. Hanke, and H. Bilz, in *Electron-Phonon Interactions and Phase Transitions,* edited by T. Riste (Plenum, New York, 1977), p. 200.
[20]W. Kress, P. Roedhammer, H. Bilz, W. D. Teuchert, and A. N. Christensen, Phys. Rev. B 17, 111 (1978).
[21]A. N. Christensen and S. Fregerslev, Acta Chem. Scand. A 31, 861 (1977).
[22]V. Ern and A. C. Switendick, Phys. Rev. 137, 1927 (1966).
[23]K. Schwarz, J. Phys. C 8, 809 (1975).
[24]A. Neckel, P. Rastl, R. Eibler, P. Weinberger, and K. Schwarz, J. Phys. C 9, 579 (1976).
[25]F. Gompf, Progress Report KFA (unpublished).
[26]W. Spengler and R. Kaiser, Solid State Commun. 18, 881 (1976).